

# A characteristic frequency of two mutually interacting gas bubbles in an acoustic field

Masato Ida

*Satellite Venture Business Laboratory, Gunma University,  
1-5-1 Tenjin-cho, Kiryu-shi, Gunma 376-8515, Japan*

---

## Abstract

Transition frequencies of two spherical gas bubbles interacting in an acoustic field are discussed theoretically. In the present study, transition frequency is defined as the frequency of external sound for which the phase difference between a bubble's pulsation and the external sound is  $\pi/2$ . It is shown by a linear theory that a bubble interacting with a neighboring bubble has three (or fewer) transition frequencies but only two natural frequencies. This result means that the bubble has a characteristic frequency besides the natural frequencies.

*Key words:* Two-bubble dynamics, Radiative interaction, Natural frequency, Phase reversal

*PACS:* 43.20.+g, 47.55.Bx, 47.55.Dz

---

It is known that radiative interaction between gas bubbles varies their natural (or resonance) frequencies, around which the bubbles indicate resonance response. This variation in the natural frequencies has been the subject of many studies [1–13]. In a case where two spherical gas bubbles of different radii interact acoustically, a bubble has two (or one) natural frequencies (see, e.g., [2,5,6,8]).

The aim of this Letter is to show that a gas bubble interacting with a neighboring bubble has an alternative characteristic frequency; we now call this a transition frequency. In the present work, a transition frequency is defined as the frequency of an external sound (the driving frequency) for which the phase difference between a bubble's pulsation and the external sound becomes  $\pi/2$ . It is well known that, in a single-bubble case, the phase difference between the bubble and an external sound becomes  $\pi/2$  when the driving frequency is equal to the bubble's natural frequency [14]. However, it is shown in this Letter that, in a double-bubble case, the number of transition frequencies differs from the number of natural frequencies. This result means that the bubbles

in the latter case have a characteristic frequency that differs from the natural frequency.

First, we derive a mathematical model to use for the present investigation. This model describes the pulsation of two coupled bubbles. Since we are interested only in the qualitative natures of the transition frequencies, we use a classical theoretical model, called a coupled-oscillator or self-consistent model [10–12], although models with greater accuracy have been proposed [4,6,7,9].

A gas bubble immersed in a liquid pulsates when a sound wave is applied. The sound pressure at the bubble position drives the pulsation. When other bubbles (named “bubble 2”  $\sim$  “bubble  $N$ ”, where  $N$  is the total number of bubbles) exist near the bubble (bubble 1), the sound waves scattered by the other bubbles also drive the pulsation of bubble 1. Namely, the driving pressure acting on bubble 1,  $p_{d1}$ , is expressed as

$$p_{d1} = p_{\text{ex}} + \sum_{j=2}^N p_{s1j}, \quad (1)$$

where  $p_{\text{ex}}$  and  $p_{s1j}$  are the sound pressures of the external sound field and the scattered wave emitted by bubble  $j$ , respectively, at the position of bubble 1. When the wavelength of the external sound wave is much larger than the bubbles’ radii and the distances between the bubbles,  $p_{\text{ex}}$  can be considered spatially uniform. By assuming that the sphericity of the bubbles is thoroughly maintained and that the liquid surrounding the bubbles is incompressible, the scattered pressure can be estimated with (see, e.g., [15])

$$p_{s1j} \approx \frac{\rho}{r_{1j}} \frac{d}{dt} (R_j^2 \dot{R}_j), \quad (2)$$

where  $\rho$  is the density of the liquid,  $r_{1j}$  is the distance between the centers of bubble 1 and bubble  $j$ ,  $R_j$  is the radius of bubble  $j$ , and the over dot denotes the time derivative.

The radial oscillation of a spherical bubble in an incompressible viscous liquid is described by the RPNNP equation [16]:

$$R_1 \ddot{R}_1 + \frac{3}{2} \dot{R}_1^2 - \frac{1}{\rho} p_{w1} = -\frac{1}{\rho} p_{d1}, \quad (3)$$

$$p_{w1} = \left( P_0 + \frac{2\sigma}{R_{10}} \right) \left( \frac{R_{10}}{R_1} \right)^{3\kappa} - \frac{2\sigma}{R_1} - \frac{4\mu \dot{R}_1}{R_1} - P_0,$$

where  $P_0$  is the static pressure,  $\sigma$  is the surface-tension coefficient at the bubble surface,  $\mu$  is the viscosity of the liquid,  $\kappa$  is the polytropic exponent of the gas

inside the bubbles, and  $R_{10}$  is the equilibrium radius of bubble 1. Substituting Eqs. (1) and (2) into Eq. (3) yields

$$R_1 \ddot{R}_1 + \frac{3}{2} \dot{R}_1^2 - \frac{1}{\rho} p_{w1} = -\frac{1}{\rho} [p_{\text{ex}} + \sum_{j=2}^N \frac{\rho}{r_{1j}} \frac{d}{dt} (R_j^2 \dot{R}_j)].$$

When  $N = 2$ , this equation is reduced to

$$R_1 \ddot{R}_1 + \frac{3}{2} \dot{R}_1^2 - \frac{1}{\rho} p_{w1} = -\frac{1}{\rho} [p_{\text{ex}} + \frac{\rho}{D} \frac{d}{dt} (R_2^2 \dot{R}_2)], \quad (4)$$

where  $D = r_{12} (= r_{21})$ . Exchanging subscripts 1 and 2 yields the model equation for bubble 2:

$$R_2 \ddot{R}_2 + \frac{3}{2} \dot{R}_2^2 - \frac{1}{\rho} p_{w2} = -\frac{1}{\rho} [p_{\text{ex}} + \frac{\rho}{D} \frac{d}{dt} (R_1^2 \dot{R}_1)], \quad (5)$$

$$p_{w2} = \left( P_0 + \frac{2\sigma}{R_{20}} \right) \left( \frac{R_{20}}{R_2} \right)^{3\kappa} - \frac{2\sigma}{R_2} - \frac{4\mu \dot{R}_2}{R_2} - P_0.$$

By assuming that the time-dependent bubble radii can be represented as  $R_1 = R_{10} + e_1$ ,  $R_2 = R_{20} + e_2$ , and  $|e_1| \ll R_{10}$ ,  $|e_2| \ll R_{20}$ , Eqs. (4) and (5) are reduced to the following linear formulae:

$$\ddot{e}_1 + \omega_{10}^2 e_1 + \delta_1 \dot{e}_1 = -\frac{p_{\text{ex}}}{\rho R_{10}} - \frac{R_{20}^2}{R_{10} D} \ddot{e}_2, \quad (6)$$

$$\ddot{e}_2 + \omega_{20}^2 e_2 + \delta_2 \dot{e}_2 = -\frac{p_{\text{ex}}}{\rho R_{20}} - \frac{R_{10}^2}{R_{20} D} \ddot{e}_1, \quad (7)$$

where

$$\omega_{j0} = \sqrt{\frac{1}{\rho R_{j0}^2} \left[ 3\kappa P_0 + (3\kappa - 1) \frac{2\sigma}{R_{j0}} \right]} \quad \text{for } j = 1, 2,$$

are the partial natural (angular) frequencies of the bubbles, and

$$\delta_j = \frac{4\mu}{\rho R_{j0}^2} \quad \text{for } j = 1, 2,$$

are the damping coefficients. (In general, the damping coefficients are determined by the sum of viscous, radiation, and thermal damping [17]; we however use the above setting to simplify the following discussion.)

The system of equations (6) and (7) corresponds to that derived by Shima when  $\sigma = 0$ ,  $\delta_1 = 0$ , and  $\delta_2 = 0$  [2], and to that by Zabolotskaya when  $\sigma = 0$  [5]. This kind of system of differential equations, called the coupled-oscillator model or self-consistent model, has been used repeatedly to analyze acoustic properties of coupled bubbles [2,5,8,10–13], and has been proved to be a useful model that can provide a qualitatively accurate result despite its simple form.

Let us analyze in detail the transition frequencies of the linear coupled system. By assuming that the external sound pressure at the bubble position is written in the form of  $p_{\text{ex}} = -P_a \sin \omega t$ , a harmonic steady-state solution of the linear coupled system is given as

$$e_1 = K_1 \sin(\omega t - \phi_1), \quad (8)$$

where

$$K_1 = \frac{P_a}{R_{10}\rho} \sqrt{A_1^2 + B_1^2}, \quad (9)$$

$$\phi_1 = \tan^{-1} \left( \frac{B_1}{A_1} \right),$$

with

$$A_1 = \frac{H_1 F + M_2 G}{F^2 + G^2}, \quad (10)$$

$$B_1 = \frac{H_1 G - M_2 F}{F^2 + G^2}, \quad (11)$$

$$F = L_1 L_2 - \frac{R_{10} R_{20}}{D^2} \omega^4 - M_1 M_2,$$

$$G = L_1 M_2 + L_2 M_1, \quad H_1 = L_2 + \frac{R_{20}}{D} \omega^2,$$

$$L_1 = (\omega_{10}^2 - \omega^2), \quad L_2 = (\omega_{20}^2 - \omega^2),$$

$$M_1 = \delta_1 \omega, \quad M_2 = \delta_2 \omega.$$

Here the solution for only bubble 1 is shown. The phase difference  $\phi_1$  becomes  $\pi/2$  when

$$A_1 = 0. \quad (12)$$

It should be noted that a case in which both  $A_1$  and  $B_1$  become zero does not exist. From Eqs. (10) and (11), one obtains

$$A_1^2 + B_1^2 = \frac{H_1^2 + M_2^2}{F^2 + G^2} \left( \frac{P_a}{R_{10}\rho} \right)^2.$$

The numerator of this equation always has a nonzero value, since  $M_2 > 0$ ; this result denies the existence of a case where both  $A_1 = 0$  and  $B_1 = 0$  are true. Also, it should be noted that  $F^2 + G^2$  appearing in the denominator of Eq. (10) always has a nonzero value. When  $G = 0$ ,  $F$  is reduced to

$$F = -\frac{M_2}{M_1}L_1^2 - \frac{R_{10}R_{20}}{D^2}\omega^4 - M_1M_2.$$

This has a nonzero, negative value because  $M_2L_1^2/M_1 \geq 0$ ,  $R_{10}R_{20}\omega^4/D^2 > 0$ , and  $M_1M_2 > 0$ . This result means that no case exists where both  $F = 0$  and  $G = 0$  are true. As a consequence, Eq. (12) is reduced to

$$H_1F + M_2G = 0. \quad (13)$$

In the following, we analyze this equation.

When the damping terms in Eq. (13) are negligible (but exist), one can easily obtain the solution for this equation. By assuming that  $M_1 \approx 0$  and  $M_2 \approx 0$ , one obtains

$$H_1F \approx 0.$$

This equation can be rewritten into two independent equations:

$$F \approx L_1L_2 - \frac{R_{10}R_{20}}{D^2}\omega^4 = 0 \quad (14)$$

and

$$H_1 = L_2 + \frac{R_{20}}{D}\omega^2 = 0. \quad (15)$$

Equation (14) is the same as the theoretical formula given in Refs. [2,5] to derive the natural frequencies of a double-bubble system; namely, the transition frequencies given by this equation correspond to the natural frequencies. This

equation predicts the existence of two natural frequencies,

$$\omega_{1\pm}^2 = \frac{\omega_{10}^2 + \omega_{20}^2 \pm \sqrt{(\omega_{10}^2 - \omega_{20}^2)^2 + 4\omega_{10}^2\omega_{20}^2 \frac{R_{10}R_{20}}{D^2}}}{2\left(1 - \frac{R_{10}R_{20}}{D^2}\right)}, \quad (16)$$

and is symmetric; namely, it exchanges subscripts 1 and 2 (or 10 and 20) in this equation to reproduce the same equation. This means that the two bubbles have the same two natural frequencies. One of the natural frequencies converges to  $\omega_{10}$  and the other to  $\omega_{20}$  for  $D \rightarrow \infty$ , and the higher natural frequency rises and the lower one falls as  $D$  decreases [2,18].

The solution of Eq. (15) given for the first time is

$$\omega_1^2 = \frac{\omega_{20}^2}{1 - R_{20}/D}. \quad (17)$$

This converges to  $\omega_{20}^2$  for  $D \rightarrow \infty$ , and increases as  $D$  decreases. In contrast to Eq. (14), Eq. (15) is asymmetric ( $H_1 \neq H_2$ ); namely, this serves to break the symmetry of the natural frequency mentioned above. The transition frequency given by Eq. (17) is not the natural frequency because it cannot be given by the natural frequency analysis performed in Refs. [2,5]. (Even the other models used in, e.g., [6,8] give only two natural frequencies.)

The results given above show that, when the damping effect is negligible and the radii of bubbles are not equal, the bubbles have three asymmetric transition frequencies; one of these, for  $D \rightarrow \infty$ , converges to the partial natural frequency of a corresponding bubble, while the remaining two converge to that of a neighboring bubble. (In the following, the former transition frequency is called “fundamental transition frequency” (FTF), and the latter two are called “sub transition frequencies” (STFs).) One of the STFs always increases as bubbles approach each other. The other STF decreases (increases) and the FTF increases (decreases) when the partial natural frequency of the bubble is higher (lower) than that of the neighboring bubble.

Figure 1 shows the transition frequencies for  $\mu \approx 0$  as a function of  $l = D/(R_{10} + R_{20})$ . Other parameters are set to  $\rho = 1000 \text{ kg/m}^3$ ,  $P_0 = 1 \text{ atm}$ ,  $\sigma = 0.0728 \text{ N/m}$ , and  $\kappa = 1.4$ . Equations (16) and (17) are used in plotting those graphs. The radius of bubble 1 is fixed to  $10 \text{ }\mu\text{m}$  and that of bubble 2 varies from  $5 \text{ }\mu\text{m}$  to  $10 \text{ }\mu\text{m}$ . As discussed above, three transition frequencies changing with  $D$  appear in each graph, except for the case of  $R_{10} = R_{20}$ , where only one decreasing transition frequency appears. (When the two bubbles have

the same radii and pulsate in phase, Eq. (6) is reduced to

$$\left(1 + \frac{R_{10}}{D}\right) \ddot{e}_1 + \omega_{10}^2 e_1 + \delta_1 \dot{e}_1 = -\frac{p_{\text{ex}}}{\rho R_{10}}.$$

This equation has only one transition frequency [5,10] of

$$\omega_1^2 = \frac{\omega_{10}^2}{1 + R_{10}/D}, \quad (18)$$

which converges to  $\omega_{10}^2$  for  $D \rightarrow \infty$  and decreases with decreasing  $D$ .) It is interesting to point out that the larger bubble, whose partial natural frequency is lower than that of the smaller bubble, has the highest transition frequency among all the bubbles.

Now we present numerical solutions of Eq. (13) to examine the influences of viscosity on transition frequencies. Figures 2–4 show the results obtained by using  $\mu = 1.137 \times 10^{-3}$  kg/(m s), which corresponds to the viscosity of water at room temperature. From those figures, we can observe that, as the viscous effect grows strong, i.e., the bubbles' radii become smaller, the STFs vanish gradually from the large-distance region (and sometimes from the small-distance region), and only the FTF remains. In the case of  $R_{10} = 1$   $\mu\text{m}$ , the STFs of a larger bubble disappear, and, when the bubbles are of similar size to each other, the FTF and the higher STF of a smaller bubble vanish in the small-distance region. In the case of  $R_{10} = 0.1$   $\mu\text{m}$ , it is difficult to distinguish the STFs from the FTF since only a smooth curve, decreasing almost monotonically with decreasing  $l$ , appears. (The transition frequency of the smaller bubble remaining in the small-distance region may be the lower one of the STFs.) Those results show that the influence of the mutual interaction of the bubbles on the transition frequencies depends on the viscosity of the surrounding material, and that this interaction weakens as the viscous effect strengthens, i.e., the threshold of the distance for the appearance of the STFs is shortened.

Lastly, we briefly discuss the pulsation amplitudes of the bubbles. Figure 5 shows  $\alpha_j \equiv (P_a/R_{j0}\rho)A_j$  and  $\beta_j \equiv (P_a/R_{j0}\rho)B_j$  for  $R_1 = 10$   $\mu\text{m}$ ,  $R_2 = 8$   $\mu\text{m}$ ,  $l = 3$ , and  $\mu = 1.137 \times 10^{-3}$  kg/(m s) as functions of  $\omega/\omega_{10}$ , where we set  $P_a = 0.1P_0$ . The present setting is equivalent to that used for one of the graphs shown in Fig. 2 except for  $l$ . In each graph shown in Fig. 5, we observe three reversals of the sign of  $\alpha_j$  and only two resonance responses, as expected. At the transition frequency that does not correspond to the natural frequency (the highest one of bubble 1 and the second highest one of bubble 2), no resonance response is obtained. This result confirms that the characteristic frequency given by Eq. (15) is not the natural frequency.

In summary, it was predicted in this Letter that a gas bubble interacting acoustically with a neighboring bubble has three transition frequencies that make the phase difference between the bubble's pulsation and an external sound be  $\pi/2$ , while readymade theories predict only two natural frequencies. This present result shows that, in a double-bubble case, the phase reversal of a bubble (e.g., from in-phase to out-of-phase with an external sound) can take place not only at the bubble's natural frequencies but also at some other frequency. The present theory for transition frequencies may be useful for understanding the reversal of the sign of the secondary Bjerknes force, which has so far been interpreted using only the natural frequencies [5,19–21]. (This subject is discussed in a separate paper of ours [22].) Furthermore, the present results might also affect understandings of some related subjects such as acoustic localization [23,24] and superresonances [10], previous investigations of which have employed systems containing only identical bubbles. The present theory for a double-bubble system will be verified [25] by the direct numerical simulation technique proposed in Ref. [26], and will be extended to a theory for an  $N$ -bubble system [27], where  $N$  denotes an arbitrary positive integer.

## References

- [1] M. Strasberg, J. Acoust. Soc. Am. **25**, 536 (1953).
- [2] A. Shima, Trans. ASME, J. Basic Eng. **93**, 426 (1971).
- [3] G. N. Kuznetsov and I. E. Shchekin, Sov. Phys. Acoust. **21**, 147 (1975).
- [4] J. F. Scott, J. Fluid Mech. **113**, 487 (1981).
- [5] E. A. Zabolotskaya, Sov. Phys. Acoust. **30**, 365 (1984).
- [6] Yu. A. Kobelev and L. A. Ostrovskii, Sov. Phys. Acoust. **30**, 427 (1984).
- [7] S. T. Zavtrak, Sov. Phys. Acoust. **33**, 145 (1987).
- [8] H. Takahira, S. Fujikawa and T. Akamatsu, JSME Int. J. Ser. II **32** (1989) 163.
- [9] A. S. Sangani, J. Fluid Mech. **232**, 221 (1991).
- [10] C. Feuillade, J. Acoust. Soc. Am. **98**, 1178 (1995).
- [11] Z. Ye and C. Feuillade, J. Acoust. Soc. Am. **102**, 798 (1997).
- [12] C. Feuillade, J. Acoust. Soc. Am. **109**, 2606 (2001).
- [13] P.-Y. Hsiao, M. Devaud, and J.-C. Bacri, Eur. Phys. J. E **4**, 5 (2001).
- [14] T. G. Leighton, *The Acoustic Bubble* (Academic Press, London, 1994), p.293.
- [15] R. Mettin, I. Akhatov, U. Parlitz, C. D. Ohl, and W. Lauterborn, Phys. Rev. E **56**, 2924 (1997).



- [16] W. Lauterborn, J. Acoust. Soc. Am. **59**, 283 (1976).
- [17] C. Devin, J. Acoust. Soc. Am. **31**, 1654 (1959).
- [18] M. Ida, e-Print, physics/0108067 (not for submission).
- [19] A. A. Doinikov and S. T. Zavtrak, Phys. Fluids **7**, 1923 (1995).
- [20] A. A. Doinikov and S. T. Zavtrak, J. Acoust. Soc. Am. **99**, 3849 (1996).
- [21] A. Harkin, T. J. Kaper, and A. Nadim, J. Fluid Mech. **445**, (2001) 377.
- [22] M. Ida, (submitted); e-Print, physics/0109005.
- [23] Z. Ye and A. Alvarez, Phys. Rev. Lett. **80**, 3503 (1998).
- [24] A. Alvarez and Z. Ye, Phys. Lett. A **252**, 53 (1999).
- [25] M. Ida, e-Print, physics/0111138.
- [26] M. Ida and Y. Yamakoshi, Jpn. J. Appl. Phys. **40**, 3846 (2001).
- [27] M. Ida, (submitted); e-Print, physics/0108056.

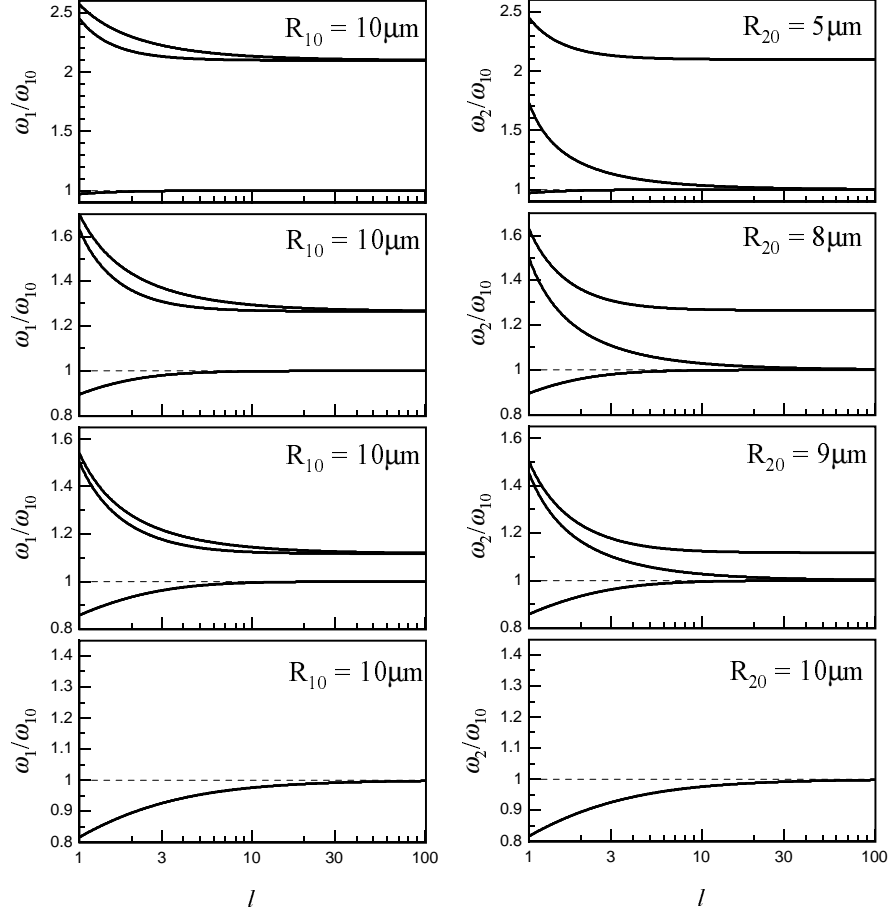


Fig. 1. Transition frequencies of bubbles 1 ( $\omega_1$ ) and 2 ( $\omega_2$ ) for  $R_{j0} \sim 10 \mu\text{m}$  and  $\mu \approx 0$ , normalized by  $\omega_{10}$ . The dashed line denotes  $\omega_j/\omega_{10} = 1$ . The highest transition frequency of bubble 1 and the second highest one of bubble 2 are given by Eq. (17).

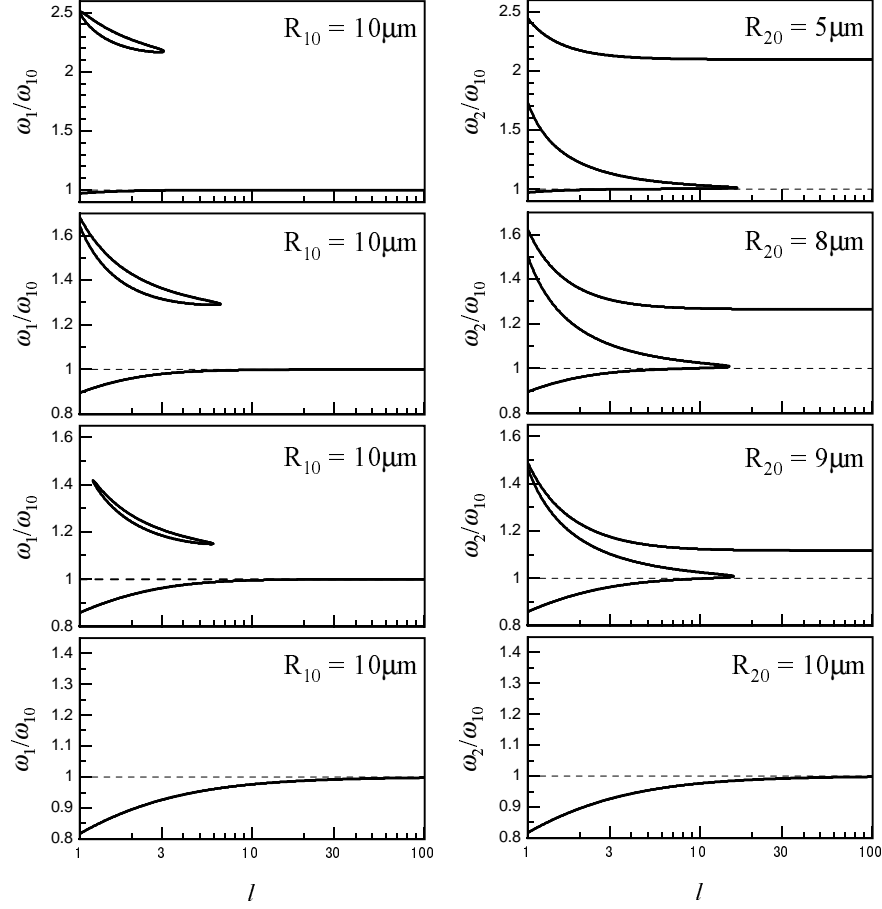


Fig. 2. Transition frequencies for  $R_{j0} \sim 10 \mu\text{m}$  normalized by  $\omega_{10}$ . The viscous effect is taken into account. The dashed line denotes  $\omega_j/\omega_{10} = 1$ .

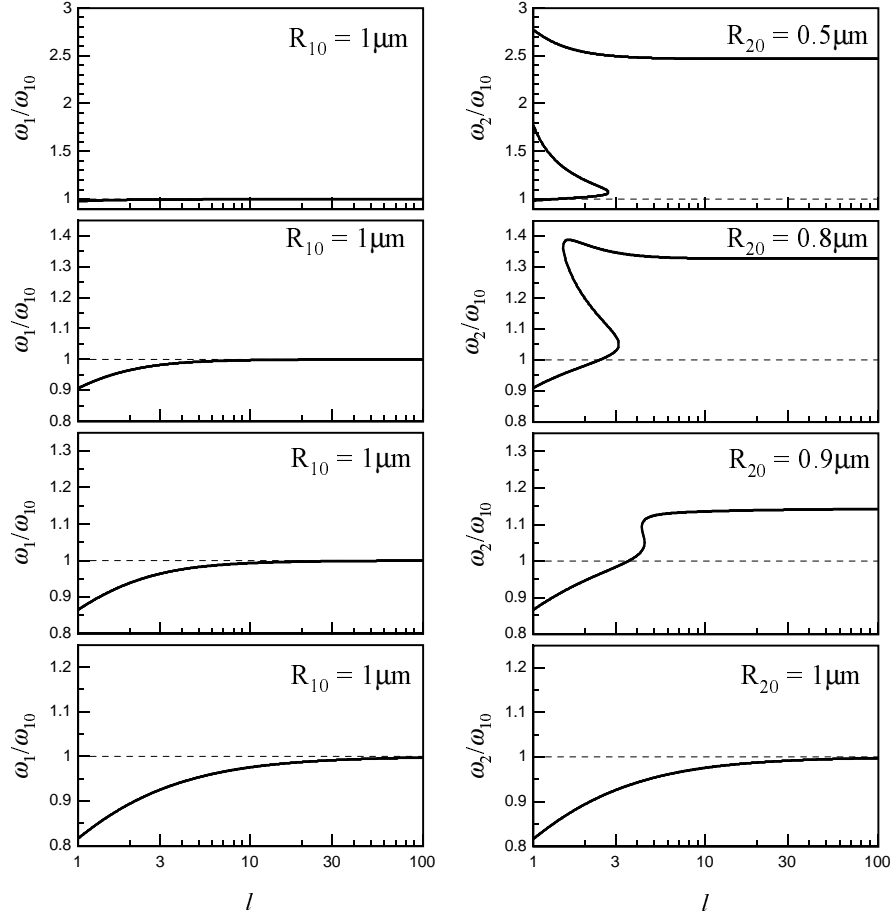


Fig. 3. Same as Fig. 2 except for  $R_{j0} \sim 1 \mu\text{m}$ .

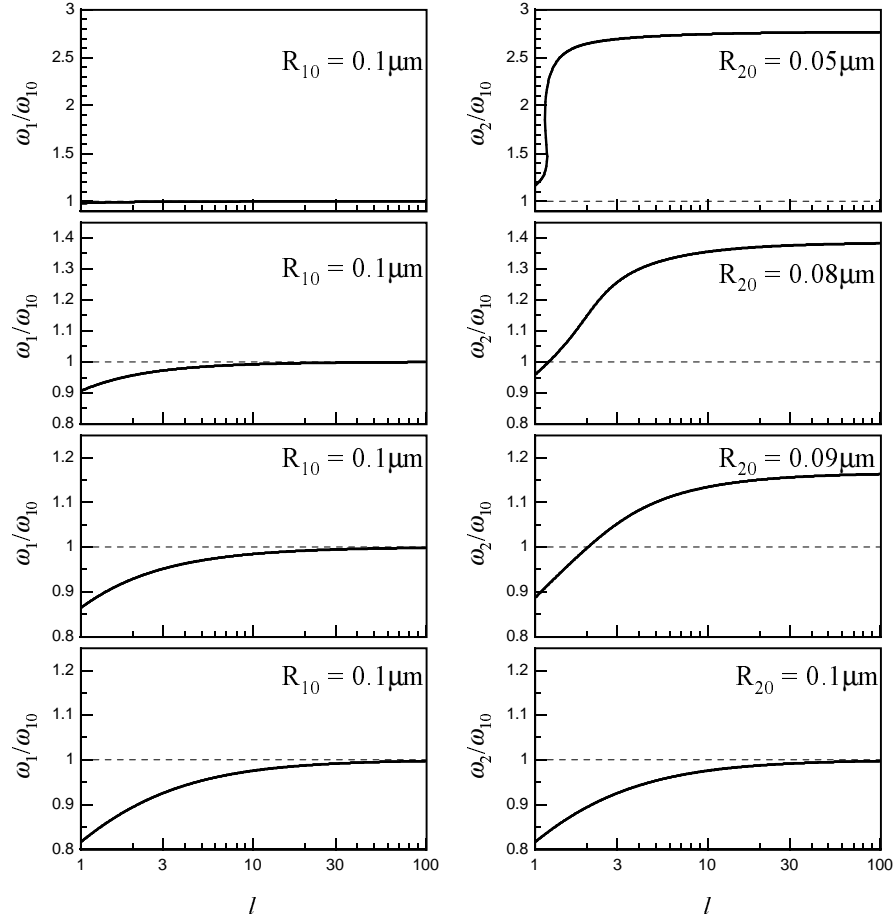


Fig. 4. Same as Fig. 2 except for  $R_{j0} \sim 0.1 \mu\text{m}$ .

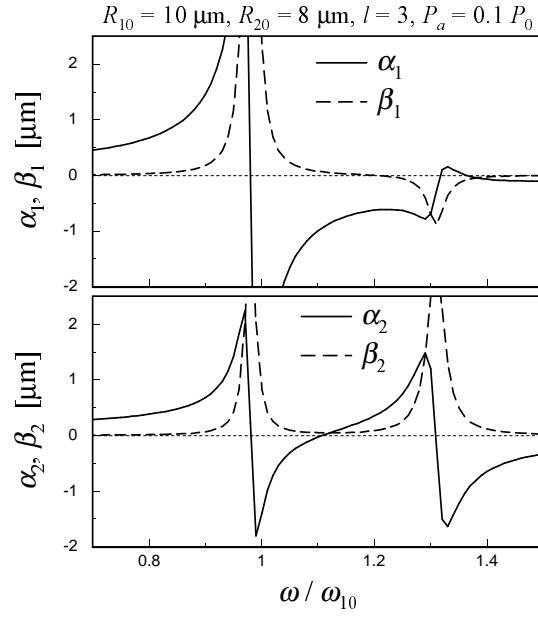


Fig. 5.  $\alpha_j = (P_a/R_{j0}\rho)A_j$  and  $\beta_j = (P_a/R_{j0}\rho)B_j$  for  $R_1 = 10 \text{ } \mu\text{m}$ ,  $R_2 = 8 \text{ } \mu\text{m}$ , and  $l = 3$ .